Contents lists available at GrowingScience

Engineering Solid Mechanics

homepage: www.GrowingScience.com/esm

A method for determination of equivalent limit load surface of fiber-reinforced nonlinear composites

Jun-Hyok Ri[a] and Hyon-Sik Hong[a*]

[a]*Institute of Mechanics, State Academy of Sciences, Pyongyang, DPR of Korea*

ARTICLEINFO

Article history:
Received 10 July, 2018
Accepted 8 October 2018
Available online
14 October 2018

Keywords:
Nonlinear homogenization
RVE
LMM
Limit analysis
Macroscopic yield surface

ABSTRACT

In this paper, a method for determining the limit load surface of fiber-reinforced nonlinear composites such as elasto-plastic composite is proposed. Using the stress approach of the homogeneous theory and the linear matching method (LMM), the limit load surface of the fiber-reinforced composite is numerically evaluated in the π- plane, and at the same time, two limit analyses determine the approximate Hill's anisotropic yield criterion for the limit load surface of the fiber-reinforced composite. The Hill's yield criterion determined by 2 limit analyses becomes the inscribed ellipse of the limit load surface evaluated numerically in the π- plane, and the limit load surface can be evaluated more accurately by the two tangent lines perpendicular to the minor axis of the inscribed ellipse and the circumscribed circle of the inscribed ellipse. This means that the limit load surface of fiber-reinforced nonlinear composite can be completely determined by only 2 limit analyses. In addition, it is found that the limit load surface is related to the equivalent strength surface of composite, and that it satisfies the Reuss and Voigt bounds.

© 2019 Growing Science Ltd. All rights reserved.

1. Introduction

It is well known that composites are extremely flexible in their application and are now increasingly used in the aerospace, automotive, and other fields since the material properties required by the designer can be easily achieved by optimizing the geometric arrangement and content of the phases constituting them (Qin & Yang, 2008). The macroscopic arrangement of the phases is considered to be statistically homogeneous. The minimum unit of this macroscopic arrangement, which can reflect the macroscopic properties of the material, is called the representative volume element (RVE). The concept of RVE created a new era for the development of composite mechanics. The macroscopic properties of heterogeneous materials can be determined by the analysis at the RVE level, and the multi-phase composite material can be regarded as the homogeneous material with macroscopic properties from the statistical homogeneity. From this, studies have been focused on the research of the problem of how the microscopic properties such as the geometric arrangement, the content and the material property of the phases constituting the composite material are related to the macroscopic properties. This problem was answered by the homogenization theory (Qin & Yang, 2008; Galvanetto & Aliabadi, 2010). Fig. 1 gives the schematic description of homogenization theory.

* Corresponding author.
E-mail addresses: honghs501@yahoo.com (H.-S. Hong)

© 2019 Growing Science Ltd. All rights reserved.
doi: 10.5267/j.esm.2018.10.002

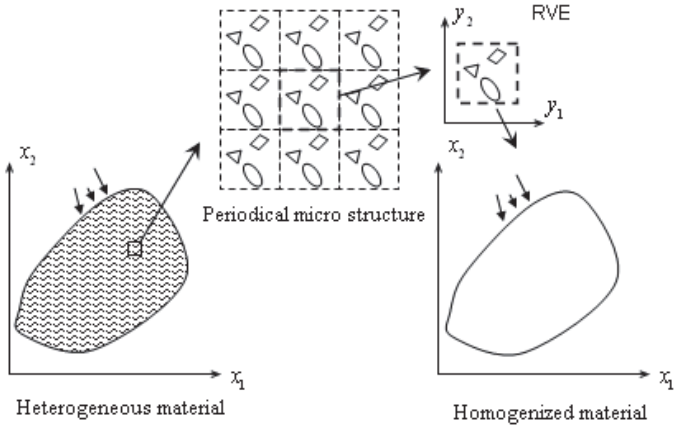

Fig. 1. Procedure for homogenization of heterogeneous material

So far, the homogenization theory of linear elastic composites has been almost completely established, but many problems remain open in the homogenization of nonlinear composites. Lastly, most of the previous studies on the homogenization of nonlinear composite material have been devoted to the evaluation of the constitutive relation of nonlinear composite material.

Secant, tangent, and generalized secant methods have been proposed to obtain the variation limits of the equivalent potential by using appropriately selected linear comparative composites (Castañeda, 1991; 1996; 2002a;b). Castañeda (1991) proposed a variational method of using linear comparison composite that was chosen optimally, and Castañeda (1996) developed the more generalized method of using the linear comparison composite by combining the tangent moduli of phases. Castañeda (2002a,b) improved the variational method by using higher-order homogenization methods. However, it is very difficult to obtain the analytical equivalent potential except for special cases (Michel & Suquet, 2003). Thus, numerical methods have been proposed to obtain the equivalent constitutive relation of composite materials including Transformation Field Analysis (TFA) and Non-uniform Transformation Field Analysis (NTFA). Michel et al. (1999), Moulinec & Suquet (1998) and Moulinec & Suquet (2003) presented a numerical method for evaluating the local and global behavior of composite materials with linear and nonlinear phases using finite element method and Fast Fourier Transforms (FFT). Michel & Suquet (2003), Michel & Suquet (2004), Lahellec & Suquet (2007) and Fritzen & Böhlke (2010) extended TFA into NTFA in consideration of non-uniform inherent strain, proposed methods for numerical implementation, and applied it to elasto-plastic composites.

Although the constitutive relation between macroscopic stress and strain of the composite material could be determined by the equivalent strain potential evaluated according to the constitutive relation and geometric arrangement of the every phase, the macroscopic strength criterion will not be determined. In practice, a detailed constitutive relation between macroscopic stress and strain is important, but macroscopic strength criterion is also of equal significance. Even though some researchers evaluated the equivalent strength surface expressed by the macroscopic stress or the strain from the limit and shakedown analysis of RVE for the elasto-plastic composites and studied the optimal design of composites based on it, their studies was restricted to the two-dimensional problem, and could not evaluate the equivalent strength surface with the low computational cost (Chen et al., 2010, 2013; Chen & Hachemi, 2014). In more detail, they numerically evaluated the equivalent limit load surface of transversely isotropic composites by two-dimensional RVE analysis, and determined the Hill's anisotropic yielding criterion by the numerical fitting based on it. Nevertheless, the macroscopic stress states cannot be placed on one π-plane with constant hydrostatic pressure since their method cannot adjust triaxial stress in the two-dimensional problem. This not only makes it impossible to reasonably select a numerical fitting point, but also to obtain the intuitive shape of limit load surface by the numerical method.

In this paper, the limit analysis of 3D RVE is carried out in order to study the case where the macroscopic stress state is placed on a π-plane with constant hydrostatic pressure. Computational points are taken on the π-plane with constant hydrostatic pressure and the corresponding macroscopic stress state is determined. Then, the limit load surface is determined numerically by calculating limit loads of fiber-reinforced composite material in the macroscopic stress states, and at the same time, an approximate Hill's anisotropic yield criterion is evaluated by two limit analyses. The Hill's anisotropic yield criterion determined from two limit analyses becomes an inscribed ellipse of the limit load surface obtained numerically, and two tangential lines perpendicular to the minor axis of inscribed ellipse and the circumscribed circle of inscribed ellipse result in more accurate evaluation of the limit load surface. Thus, the limit load surface of fiber-reinforced nonlinear composite could be completely determined by only two limit analyses. It is also shown that the limit load surface is related to the equivalent strength surface of composite material, and that the equivalent strength surface satisfies the Reuss and Voigt bounds. Every phase is assumed to be the perfectly-plastic material with the von Mises yield criterion. Stress approach is used for the homogenization boundary condition, and the Linear Matching Method is adopted for the limit analysis.

The contents of this paper are as follows. Section 2 briefly formulates the Melan's theorem and section 3 describes the algorithm of LMM. Section 4 is devoted to the explanation of the homogenization theory and the Hill's anisotropic yield criterion. The stress approach method for determining the limit load of composite material is described and the characteristics of Hill's anisotropic yield criterion is presented, and the coordinate transformation relation that conforms the yield surface onto the π-plane is derived. Some numerical results for the fiber-reinforced composite are presented in section 5. The limit load surface of fiber-reinforced composite is extracted by comparing the numerically determined limit load curves and the approximate Hill's anisotropic yield criterion for fibers with different yield stress. A few concluding remarks are mentioned in section 6.

2. Lower and upper bound theorem of limit analysis

Let us consider the limit analysis of perfectly-plastic material which follows von Mises yielding rule. It is assumed that a body occupies volume V with surface S where a traction is given as zero or $P \cdot p_i(\boldsymbol{x})$ on S_T and displacement $\bar{u}_i = 0$ is specified on S_u $(S = S_T + S_u)$. Here, P is a scalar parameter defining relative magnitude of applied load as compared with a reference load p_i. The lower and upper bound theorem of limit load can be postulated as follows, respectively (Chen & Hachemi, 2014; Ponter & Carter, 1997; Ponter et al., 2000).

Lower bound theorem:

If, for the external load $P = P_{LB}$, there exists a statically possible stress field σ_{ij}^* such that

$$f\left(\sigma_{ij}^*\right) \le \sigma_y \tag{1}$$

At every point within V, then $P_L \ge P_{LB}$. Here, f is a von Mises yield function and σ_y is a uniaxial yield stress. Thus, one can know that a maximum value of P_{LB} becomes lower bound of limit load.

Upper bound theorem:

If, for the external load $P = P_{UB}$, there exists a kinetically possible displacement rate field $\dot{u}_i^*$ and its corresponding strain rate field $\dot{\varepsilon}_{ij}^*$ such that

$$P_{UB} \int_{S_T} p_i \dot{u}_i^* = \int_V \sigma_{ij}^{P^*} \dot{\varepsilon}_{ij}^* dV \,, \tag{2}$$

where σ_{ij}^{p*} is a stress point at yield associated with $\dot{\varepsilon}_{ij}^{*}$, then satisfies $P_L \le P_{UB}$. Hence, one can know that a minimum value of P_{UB} becomes upper bound of limit load.

3. Linear matching method (LMM)

The LMM is based on the linear elastic finite element analysis (FEA) with spatially varying material properties (Ponter & Carter, 1997; Fuschi & Engelhardt, 2000; Chen & Ponter, 2001). LMM has been successfully applied to the limit and shakedown analysis of structures subjected to heating and inner pressure and composites. Chen (2010a,b), and Cho & Chen (2018) presented the numerical value implementation of LMM by using ABAQUS user subroutine UMAT, and applied the LMM to the shakedown analysis of structure subjected to the cyclic heating and mechanical load. Pisano & Fuschi (2007), Pisano & Fuschi (2011) and Pisano et al. (2013) evaluated the strength of fiber-reinforced laminates by formulating and implementing the LMM for orthotropic composites. For the LMM, the Young's modulus is changed spatially such that stress field corresponding to a certain kinetically possible strain field is placed on the yielding surface at every point of material. The Poisson ratio is taken as 0.4999999 since material is considered to have plastic incompressibility. LMM algorithm could be formulated as follows (Ponter & Carter, 1997; Ponter et al., 2000; Chen & Ponter, 2001).

- Initialization: Set $P_{UB}^{0}=1,\ E^{1}(\mathbf{x})=E$.
- k th iteration:

The linear elastic analysis with the Young's modulus of $E^{k}(\mathbf{x})$ is performed under a load $P_{UB}^{k-1}\cdot p$ and σ_{ij}^{k}, ε_{ij}^{k} and u_i^{k} is obtained, respectively.

Lower and upper bound of the limit load at k th iteration is evaluated as

$$P_{LB}^{k}=P_{UB}^{k-1}\frac{\sigma_y}{\sigma_{eq}\left(\sigma_{ij}^{k}\right)}, \tag{3}$$

$$P_{UB}^{k}=P_{UB}^{k-1}\frac{\int_V \sigma_y \varepsilon_{eq}\left(\varepsilon_{ij}^{k}\right)}{\int_{S_T} P_{UB}^{k-1} p_i u_i^{k}}, \tag{4}$$

where, σ_{eq} and ε_{eq} denotes equivalent stress and equivalent strain, respectively.

E^{k+1} at $k+1$ th iteration is updated as follows.

$$E^{k+1}=\frac{\sigma_y}{\varepsilon_{eq}\left(\varepsilon_{ij}^{k}\right)}\ . \tag{5}$$

Eq. (5) gives E^{k+1} at $k+1$ th iteration such that stress field corresponding to strain field ε_{ij}^{k} obtained at k th iteration lies on the yielding surface. Nevertheless, for high gradient of stress, Young's modulus evaluated by Eq. (5) may not give stable solution, sometimes. In order to overcome this numerical difficulty without any affection on LMM solution, we do the normalization using initial Young's modulus E_{ref} of material.

We denote a minimum value of Young's modulus $E^{k}(\mathbf{x})$ on whole region obtained at $k-1$ th iteration by $E_{\min}^{k}=\min_{\mathbf{x}} E^{k}(\mathbf{x})$. Then, after performing k th iteration, E^{k+1} at $k+1$ th iteration will be evaluated by

$$E^{k+1} = \frac{E_{ref}}{E^k_{\min}} \frac{\sigma_y}{\varepsilon_{eq}\left(\varepsilon^k_{ij}\right)}, \tag{6}$$

instead of using Eq. (5). Even though Eq. (6) shows a theoretical equivalence with Eq. (5), our computational experiences ensure that Eq. (6) can improve the numerical stability much more as compared with Eq. (5) (Ri & Hong, 2017).

The LMM gives a set of non-increasing upper bounds of the limit load, but occasionally it may not give a set of non-decreasing lower bounds for the lower bound. There is a method to use the following Eq. (7), instead of using Eq. (5), which is called an Elastic Compensation Method (ECM) (Pisano & Fuschi, 2011; Pisano & Fuschi, 2013; Ri & Hong, 2017).

$$E^{k+1} = \begin{cases} E & \sigma_{\text{eq}}\left(\sigma^k_{ij}\right) < \sigma_y \\ \dfrac{\sigma_y}{\varepsilon_{eq}\left(\varepsilon^k_{ij}\right)} & \sigma_{\text{eq}}\left(\sigma^k_{ij}\right) \geq \sigma_y \end{cases} \tag{7}$$

Although the ECM gives both a set of non-increasing upper bounds and a set of non-decreasing lower bounds, the convergence rate of upper bound set cannot be faster than the LMM. In fact, the ECM was developed earlier than the LMM, but now it is used as a complementary method to the LMM that is perfect theoretically. Moreover, since LMM and ECM differ only in whether the Young's modulus is changed by Eq. (6) or Eq. (7) in the iteration process, the upper bound of limit load is evaluated by the LMM and the lower bound by the ECM, without a special distinction of both methods in this paper. The limit analysis is performed using the UserMat subroutine of the commercial software ANSYS.

4. Homogenization theory and anisotropic yield condition

The mechanical behavior of composite materials could be considered on two scales, macroscopic one x and microscopic one y. Macroscopic scale and microscopic one have the following relation (Qin & Yang, 2008; Galvanetto & Aliabadi, 2010).

$$y = x/\delta . \tag{8}$$

Here, δ is a material parameter reflecting the size of RVE. The stress and strain on the macroscopic scale are defined as the volume average of microscopic stress and strain on RVE, respectively. Namely,

$$\bar{\sigma}_{ij} = \frac{1}{V_R}\int_{\Omega_R} \sigma_{ij} dV = \left\langle \sigma_{ij} \right\rangle , \tag{9}$$

$$\bar{\varepsilon}_{ij} = \frac{1}{V_R}\int_{\Omega_R} \varepsilon_{ij} dV = \left\langle \varepsilon_{ij} \right\rangle , \tag{10}$$

where V_R is the volume of RVE.

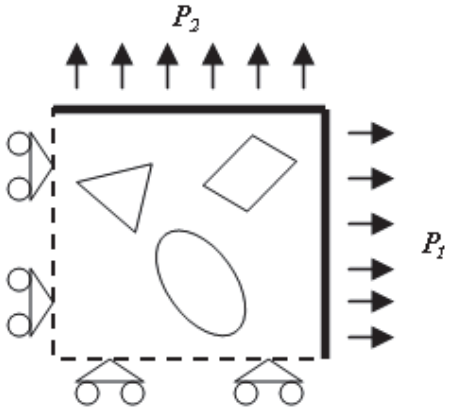

Fig. 2. Boundary condition of stress approach

On the boundary of RVE, the periodic boundary condition must be satisfied. There are various methods depending on which periodic boundary conditions are satisfied. However, the stress approach shown in Fig. 2 is used in this paper because it is necessary to obtain the equivalent strength surface in the stress space. The use of strain or displacement approach requires the transformation of equivalent strength surface onto the stress space because it is expressed in terms of strain or displacement. Furthermore, it may require the supplementary nonlinear homogenization due to the nonlinearity of constitutive relation.

Even though the equivalent strength of composite can be determined experimentally, the experimental method is not suitable for evaluating the strength of composite materials at the design stage, in particular. Thus, the strength of the composite material will be numerically evaluated by combining the limit analysis and the Hill's anisotropic yield criterion in this paper. For this, we consider the Hill's anisotropic yield criterion in the principal stress space as follows,

$$F(\sigma_2-\sigma_3)^2+G(\sigma_3-\sigma_1)^2+H(\sigma_1-\sigma_2)^2=1. \tag{11}$$

Here,

$$\begin{aligned} F&=\frac{1}{2}\left(\frac{1}{Y^2}+\frac{1}{Z^2}-\frac{1}{X^2}\right),\\ G&=\frac{1}{2}\left(\frac{1}{Z^2}+\frac{1}{X^2}-\frac{1}{Y^2}\right),\\ H&=\frac{1}{2}\left(\frac{1}{X^2}+\frac{1}{Y^2}-\frac{1}{Z^2}\right), \end{aligned} \tag{12}$$

where the principal stress space, Eq. (11) represents the elliptic cylindrical surface parallel to the hydrostatic pressure axis. Thus, the yield surface is represented by a closed curve in the π-plane perpendicular to the hydrostatic axis. Let us denote the coordinate system of the principal stress space by $(o-xyz)$. When the coordinate system is rotated so that the coordinate axis z coincides with the hydrostatic pressure axis, the yield surface becomes a single curve on the rotated xy plane, and the stresses γ_1, γ_2 and γ_3 in the rotated coordinate system have the following relation with the principal stresses σ_1, σ_2 and σ_3, respectively.

$$\gamma_1=0.7877\sigma_1-0.2113\sigma_2+0.5774\sigma_3,$$

$$\gamma_2 = -0.2113\sigma_1 + 0.7877\sigma_2 + 0.5774\sigma_3,$$
$$\gamma_3 = 0.5774(\sigma_1 + \sigma_2 + \sigma_3). \tag{13}$$

Eq. (11) will be expressed as follows in the rotated coordinate system.

$$(0.134F + 1.866G + H)\gamma_1^2 + (1.866F + 0.134G + H)\gamma_1^2 + (F + G - 2H)\gamma_1\gamma_2 = 1. \tag{14}$$

In case of fiber reinforcement, e.g. $X = Y$, and $F = G = \frac{1}{2Z^2}$, Eq. (11) is represented as follows,

$$(2F + H)\gamma_1^2 + (2F + H)\gamma_1^2 + (2F - 2H)\gamma_1\gamma_2 = 1, \tag{15}$$

where Eq. (15) denotes the equation of ellipse whose the major axis and minor axis are inclined by 45^0 with respect to the coordinate axis, respectively. The major radius *a* and the minor radius *b* are expressed as follows,

$$H = \frac{1}{2a^2} - \frac{1}{6b^2},$$
$$F = \frac{1}{3b^2}. \tag{16}$$

5. Numerical example

In this section, the fiber-reinforced metal matrix composite is considered. Both the matrix and the reinforcement is assumed to be perfectly-plastic material. In the case of the base material and the reinforcement being the same homogeneous material, the yield condition is reduced to the von Mises yield criterion. We assume that the yield stress of the matrix is 80 MPa, and that the ratio k of yield stress σ_m of matrix to yield stress σ_f of reinforcement is 1 to 25. Fig. 3 shows the finite element (FE) model of RVE used for the limit analysis. The Hill's yield criterion is completely determined once only 2 parameters $X = Y$, Z are known. We determine the Hill's yield criterion by extracting parameters $X = Y$, Z from the limit analyses under the tension or compression in the x and z-direction. The major radius and the minor radius on the π-plane are determined from Eq. (16). For convenience, we will simply call the Hill's yield criterion evaluated by 2 limit analyses as the Hill's yield criterion. Meanwhile, limit analyses corresponding to different macroscopic stress states are carried out in order to evaluate the limit load surface numerically, which is simply referred to the limit load surface.

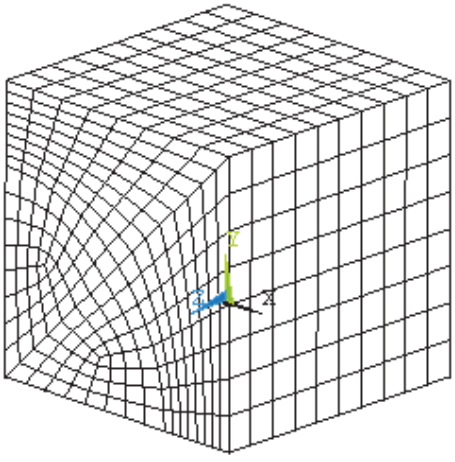

Fig. 3. FE model of RVE used for limit analysis

Fig. 4 shows predicted results for different values of k. As shown in this Figure, the Hill's yield criterion becomes the inscribed ellipse of the limit load surface in all cases, so that it provides the safe approximation of the limit load surface.

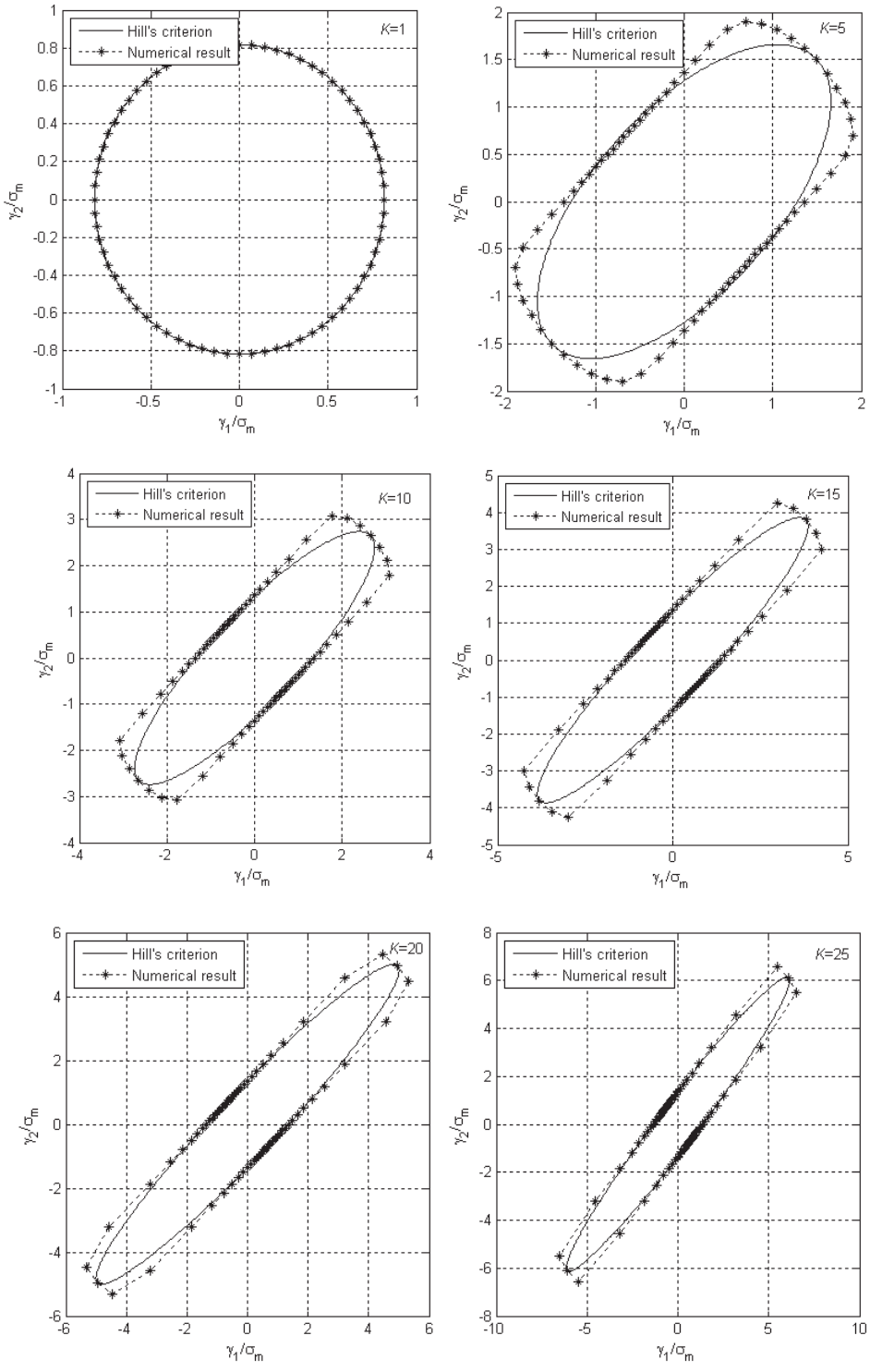

Fig. 4. Predicted results of Hill's yield criterion and limit load surface for different values of k

In order to obtain a more accurate approximation of the limit load surface, a tangent line perpendicular to the minor axis and the circumscribed circle of the Hill's yield criterion is drawn as seen from Fig. 5a for case of $k = 10$. Results are similar for cases with different values of k (Fig. 5b).

From Fig. 5, it can be seen that the limit load surface of the material can be approximated accurately by two straight lines and two arcs. Therefore, it could be concluded that the Hill's yield criterion obtained from only two limit analyses can predict the limit load surface with sufficient accuracy.

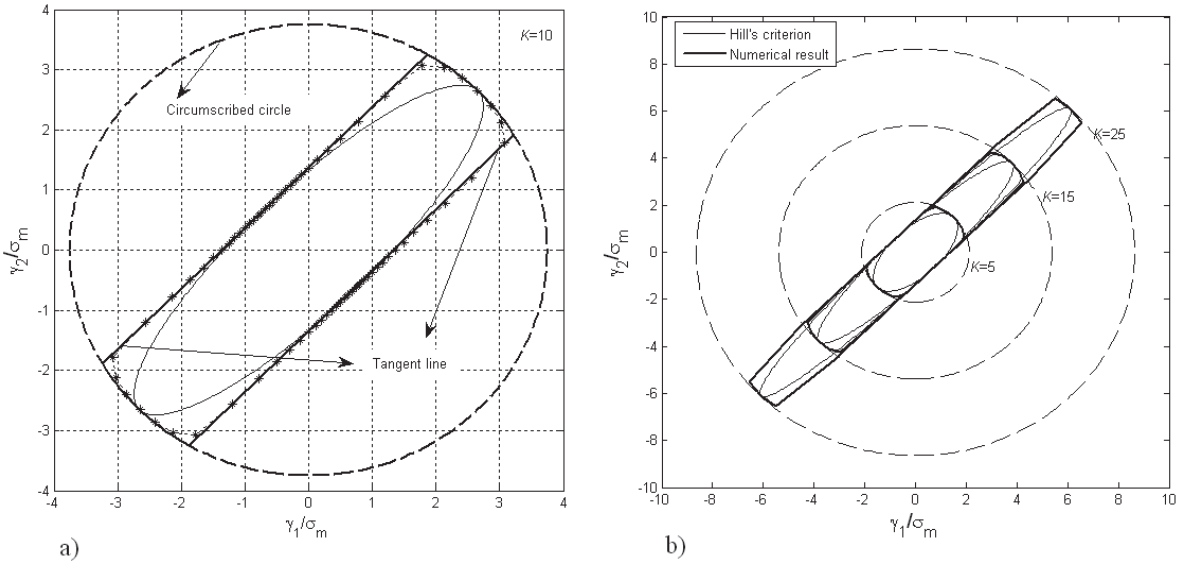

Fig. 5. Approximation of limit load surface: a) $k=10$; b) $k=5$, 15, 25

In order to consider the influence of the yield stress of reinforcement on the strength, Fig. 6 shows the comparison of the Hill's yield criterion corresponding to different values of k as well as the change of the major and minor radius varying with the yield stress of reinforcement. As shown from figure 6, while the major radius of yield curve on the π-plane continues to increase linearly, the minor radius stops to increase when the yield stress of reinforcement increases 5 times or more than the yield stress of the matrix. This means that the effect of reinforcement is the weakest when $\sigma_x = \text{-}\sigma_y$ corresponding to the minor axis and the strongest when $\sigma_x = \sigma_y$ corresponding to the major axis.

Next, the comparison with different analytical approximations is performed. The equivalent strength surface P^{hom} of the composite made of the perfectly-plastic material could be represented as follows (Ponte Castañeda, 2002).

$$P^{\text{hom}} = \left\{\overline{\sigma}; \langle\sigma\rangle = \overline{\sigma}, div(\sigma(y)) = 0, \sigma_{eq}(y) \le \sigma_0(y)\right\} \tag{17}$$

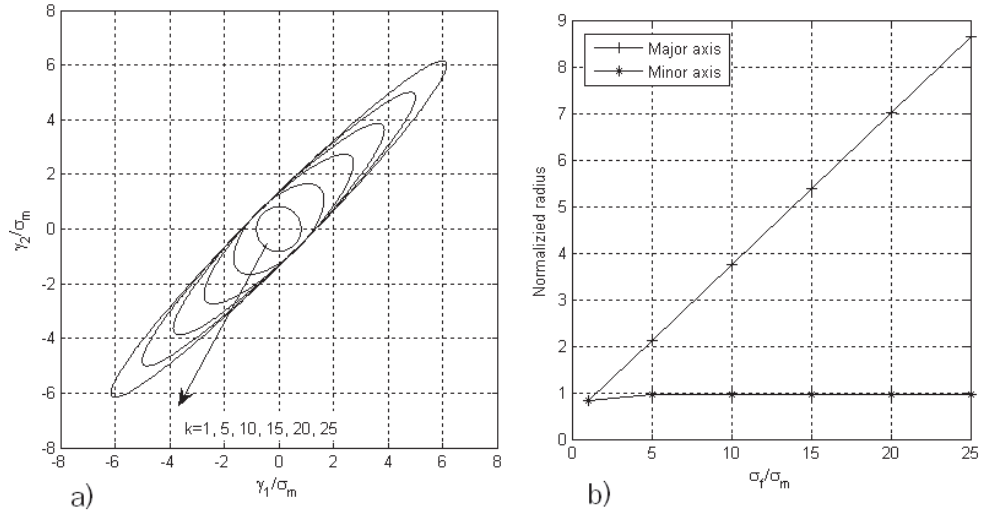

Fig. 6. a) Hill's yield criterion for different values of k; b) Change of major and minor radius with yield stress of reinforcement

We get important conclusion from the lower bound theorem of limit load that the equivalent strength surface $P^{\hom}$ eventually becomes the limit load surface of the RVE and that the equivalent strength surface $P^{\hom}$ can also be determined by using the upper bound theorem of the limit load from the duality of limit load. Now, let us focus on the following relation, rather than Eq. (17).

$$\left\{\overline{\sigma}, \overline{\sigma}_{eq} \le \inf_{y \in V_R} \sigma_0(y)\right\} \subset P^{\hom} \subset \left\{\overline{\sigma}, \overline{\sigma}_{eq} \le \langle \sigma_0 \rangle\right\}. \tag{18}$$

The left and right sides of Eq. (18) denote the Reuss and Voigt bound of the equivalent strength surface, respectively. For the Reuss lower bound, $f(\overline{\sigma}) \le \sigma_m$ due to $\sigma_m \le \sigma_f$ while $f(\overline{\sigma}) \le (1 - V_f)\sigma_m + V_f \sigma_f$ for the Voigt upper bound. Fig. 7 shows the limit load surface, the Reuss lower bound and the Voigt upper bound for different values of k.

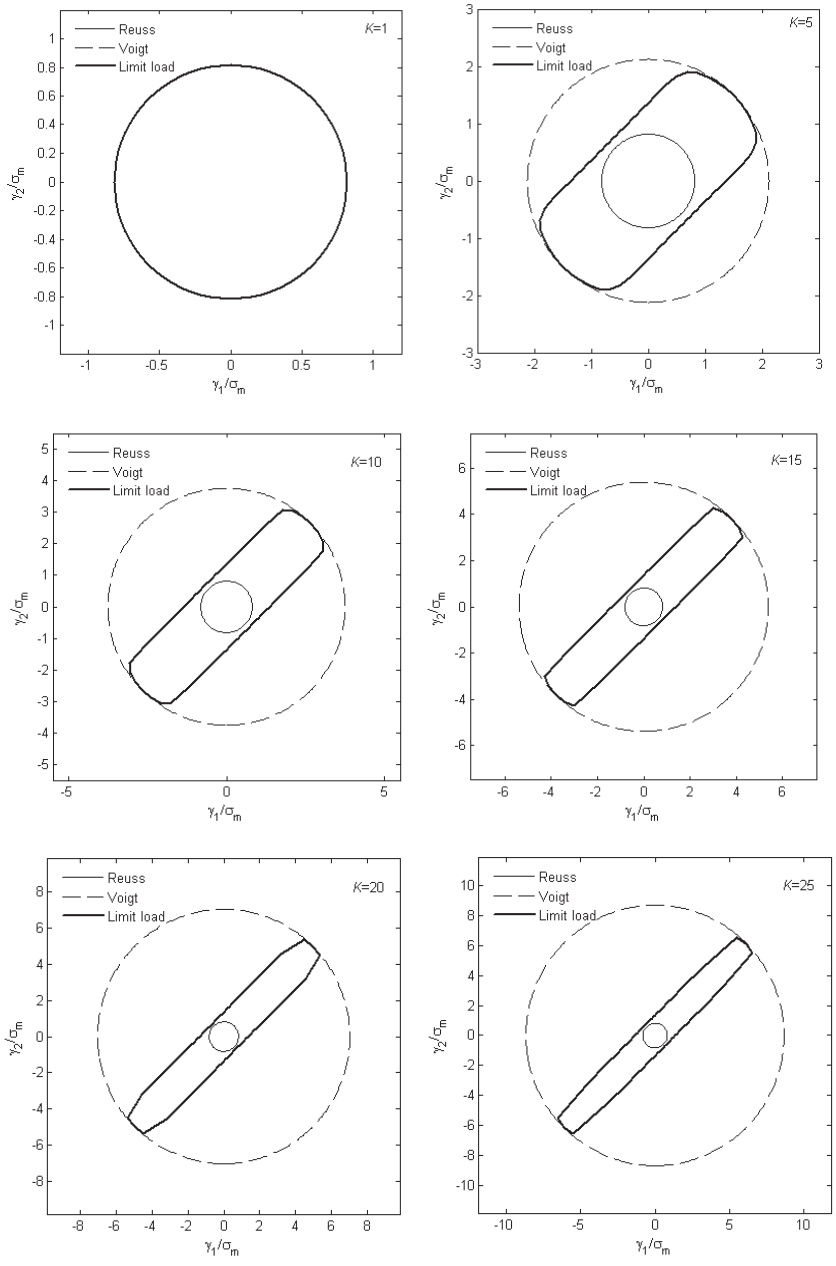

Fig. 7. Limit load surface, Reuss lower bound and Voigt upper bound for different values of k

It is easy to see that the limit load surface obtained by the limit analysis satisfies Eq. (18) from Fig. 7. Since $k=1$ corresponds to the homogeneous material, the limit load surface, the Reuss lower bound and the Voigt upper bound exactly the same.

5. Conclusion

In this paper, we proposed a simple method for determining the limit load surface of fiber-reinforced composites. Based on the assumption that the limit load surface can be approximated by the Hill's anisotropic yield criterion, Hill's anisotropic yield criterion is predicted by two limit analyses on the three dimensional RVE and compared with the numerically evaluated limit load surface. The limit loads in the macroscopic stress space are evaluated by the limit analysis of RVE using the stress approach of the homogenization theory and the LMM. The Hill's yield criterion determined by two limit analyses becomes the inscribed ellipse of the limit load surface evaluated numerically in the π-plane, and the limit load surface can be evaluated more accurately by the two tangent lines perpendicular to the minor axis of the inscribed ellipse and the circumscribed circle of the inscribed ellipse. This means that the limit load surface of fiber-reinforced nonlinear composite can be completely determined by only two limit analyses. In addition, it is found that the limit load surface is related to the equivalent strength surface of composite, and that it satisfies the Reuss and Voigt bounds.

References

Castañeda, P. P. (1991). The effective mechanical properties of nonlinear isotropic composites. *Journal of the Mechanics and Physics of Solids*, *39*(1), 45-71.

Castañeda, P. P. (1996). Exact second-order estimates for the effective mechanical properties of nonlinear composite materials. *Journal of the Mechanics and Physics of Solids*, *44*(6), 827-862.

Castañeda, P. P. (2002a). Second-order homogenization estimates for nonlinear composites incorporating field fluctuations: I—theory. *Journal of the Mechanics and Physics of Solids*, *50*(4), 737-757.

Castañeda, P. P. (2002b). Second-order homogenization estimates for nonlinear composites incorporating field fluctuations: II—applications. *Journal of the Mechanics and Physics of Solids*, *50*(4), 759-782.

Castañeda, P. P., Telega, J. J., & Gambin, B. (Eds.). (2006). *Nonlinear Homogenization and its Applications to Composites, Polycrystals and Smart Materials: Proceedings of the NATO Advanced Research Workshop, held in Warsaw, Poland, 23-26 June 2003* (Vol. 170). Springer Science & Business Media.

Chen, H. F., & Ponter, A. R. (2001). Shakedown and limit analyses for 3-D structures using the linear matching method. *International Journal of Pressure Vessels and Piping*, *78*(6), 443-451.

Chen, M., & Hachemi, A. (2014). *Progress in Plastic Design of Composites, in: Spiliopoulos, K., Weichert, D. (Eds), Direct Methods for Limit States in Structures and Materials*. Springer, Dordrecht, pp 119-138.

Chen, M., Hachemi, A., & Weichert, D. (2010). A non-conforming finite element for limit analysis of periodic composites. *PAMM*, *10*(1), 405-406.

Chen, H. (2010a). Lower and upper bound shakedown analysis of structures with temperature-dependent yield stress. *Journal of Pressure Vessel Technology*, *132*(1), 011202.

Chen, H. (2010b). Linear matching method for design limits in plasticity. *Computers, Materials and Continua-Tech Science Press*, *20*(2), 159-183.

Chen, M., Hachemi, A., & Weichert, D. (2013). Shakedown and optimization analysis of periodic composites. In *Limit State of Materials and Structures* (pp. 45-69). Springer, Dordrecht.

Cho, N. K., & Chen, H. (2018). Shakedown, ratchet, and limit analyses of 90° back-to-back pipe bends under cyclic in-plane opening bending and steady internal pressure. *European Journal of Mechanics-A/Solids*, *67*, 231-242.

Fritzen, F., & Böhlke, T. (2010). Three-dimensional finite element implementation of the nonuniform transformation field analysis. *International Journal for Numerical Methods in Engineering*, *84*(7), 803-829.

Galvanetto, U., & Aliabadi, M. H. (2010). *Multiscale modeling in solid mechanics: computational approaches* (Vol. 3). World Scientific.

Lahellec, N., & Suquet, P. (2007). On the effective behavior of nonlinear inelastic composites: I. Incremental variational principles. *Journal of the Mechanics and Physics of Solids*, *55*(9), 1932-1963.

Michel, J. C., Moulinec, H., & Suquet, P. (1999). Effective properties of composite materials with periodic microstructure: a computational approach. *Computer methods in applied mechanics and engineering*, *172*(1-4), 109-143.

Michel, J. C., & Suquet, P. (2003). Nonuniform transformation field analysis. *International journal of solids and structures*, *40*(25), 6937-6955.

Michel, J. C., & Suquet, P. (2004). Computational analysis of nonlinear composite structures using the nonuniform transformation field analysis. *Computer methods in applied mechanics and engineering*, *193*(48-51), 5477-5502.

Moulinec, H., & Suquet, P. (1998). A numerical method for computing the overall response of nonlinear composites with complex microstructure. *Computer methods in applied mechanics and engineering*, *157*(1-2), 69-94.

Moulinec, H., & Suquet, P. (2003). Intraphase strain heterogeneity in nonlinear composites: a computational approach. *European Journal of Mechanics-A/Solids*, *22*(5), 751-770.

Pisano, A. A., & Fuschi, P. (2007). A numerical approach for limit analysis of orthotropic composite laminates. *International journal for numerical methods in engineering*, *70*(1), 71-93.

Pisano, A. A., & Fuschi, P. (2011). Mechanically fastened joints in composite laminates: Evaluation of load bearing capacity. *Composites Part B: Engineering*, *42*(4), 949-961.

Pisano, A. A., Fuschi, P., & De Domenico, D. (2013). Peak load prediction of multi-pin joints FRP laminates by limit analysis. *Composite Structures*, *96*, 763-772.

Ponter, A. R. S., & Carter, K. F. (1997). Limit state solutions, based upon linear elastic solutions with a spatially varying elastic modulus. *Computer Methods in Applied Mechanics and Engineering*, *140*(3-4), 237-258.

Ponter, A. R., Fuschi, P., & Engelhardt, M. (2000). Limit analysis for a general class of yield conditions. *European Journal of Mechanics-A/Solids*, *19*(3), 401-421.

Qin, Q. H., & Yang, Q. S. (2008). *Macro-micro theory on multi-field coupling behavior of heterogeneous materials*. Springer,.

Ri, J. H., & Hong, H. S. (2017). A modified algorithm of linear matching method for limit analysis. *Archive of Applied Mechanics*, *87*(8), 1399-1410.

© 2018 by the authors; licensee Growing Science, Canada. This is an open access article distributed under the terms and conditions of the Creative Commons Attribution (CC-BY) license (http://creativecommons.org/licenses/by/4.0/).